Comparison between polymer processing aids in extrusion of polyolefin films

Mónica Sofia Almeida, António Correia Diogo[1], Maria Helena Sousa[2]
[1]Departamento de Engenharia Química, Instituto Superior Técnico
[2]Isolago,SA

Abstract

The polymer processing aids are used to avoid the formation of flow instabilities during the extrusion of polyolefins, this way it increases the productivity and quality of the finals products.

This thesis presents a comparative study of three polymer processing aids, PPA-1, PPA-2 and PPA-3, made of fluoropolymers and the characterization of the defects of the extruded polymer, like sharkskin and gel. To determine which formulation works better, linear low density polyethylene was processed with the PPA, in blown film extruder and capillary extruder. The defects observed in the film were characterized by optic microscopy, electronic microscopy and Dynamic Mechanical Analysis (DMA) in a dynamic regime and a transitory regime.

The composition of the formulations used were analysed by infrared spectroscopy. In particular, it was verified that the composition of PPA-3 it's different than PPA-1 and PPA-2 because the first has more quantity of vinylidene fluoride on fluoropolymers.

The determination of the birefringence in the film with gel, done by optic microscopy, allowed to verify that in the defect the polymer chains are under pressure. Through electronic microscopy it as confirmed that the structure of "sharkskin" is associated to the phenomenon of elastic recovery of the polymer. The analysis of the rheological behaviour of the films, done by DMA, shows that the film with "sharkskin" has less resistance to deformation. On the other hand, the films with gel have major resistance to deformation, when compared with films with smooth surface. The results show that the formulation PPA-1 is more efficient, thereafter the formulation PPA-2 and PPA-3.

Keywords: Polymer processing aids, fluoropolymers, linear low density polyethylene, film and sharkskin.

1. Introduction

The thermoplastic melt flow through a die is stable at for low values of pressure gradient or flow rate. When a pressure gradient or flow rate increases may occur flow instabilities. This affects the surface and/or the cross section and the mechanical properties of the extrudate.

In the beginning the flow instabilities occurs to low values of flow rate, allowing the development of additives, usually named as polymers processing aids (PPA). These increases the beginning of the flow instabilities, resulting in increased productivity of the extrusion line. The PPA usually used are based in fluoropolymers.

The flow instabilities appear during the extrusion of LLDPE. Nowadays this type of polyethylene is becoming more widely used as a substitute of low density polyethylene, LDPE. As LLDPE generally has better mechanical properties than LDPE, like tensile strength and percent elongation.

The causes and microscopic mechanisms related to flow instabilities are not yet completely known. The flow instabilities are still under studies in order to improve the PPA composition and the how to use the PPA. It is known that surface defects are originated close to the die exit and can corresponds to micro-roughness and macro-roughness, like sharkskin or orange skin. The body defects (cross section) were originated close to the entrance of the die. They can be divided in stick-slip, super-extrusion and gross melt fracture.

The sharkskin on polymer extrudate was the defect analysed in this study and corresponds to periodical distortions of small amplitude [1,2]. According to Hatzikiriakos e Migler [1] the origin of sharkskin is related to the acceleration of the extrudate surface after the extrusion die. The polymer melt flow has zero velocity at the die wall and maximum velocity at the center. So at the die exit the extrudate surface accelerates in order to follow up the velocity of the center. If the critical wall shear stress is exceeded, the rapid acceleration of the surface extrudate may induce local traction stresses. The relaxation of such stresses causes periodical distortions at the surface of the extrudate, this means sharkskin. Using PPA the local traction stresses at the die exit does not arise.

During the processing of LLDPE with PPA, the PPA particles are deposited in the die wall and form a layer. This occurs because the fluoropolymers has high affinity with the material

of the die wall and low affinity with the polyethylene. So the PPA particles migrate from the center of polymer melt until the die wall. The formation of a die coating allows decreasing the entangled density of polymer chains at the surface. As a result, the flow velocity at the wall increases and the wall shear stress decreases. Also the critical flow rate increases. This means that the flow instabilities will appear at high flow rate. Consequently the pressure decreases and the extrudate polymer does not have defects. Furthermore PPA reduces gels formation and die build up.

The PPA efficiency is related with time to eliminate sharkskin and pressure reduction. The lower the time to eliminate sharkskin, the higher the efficiency. The higher the pressure reduction and faster the stabilization of pressure, more efficient is the PPA [1,2].

According to Kulikov [3-5] the fluoropolymers have two high disadvantages: the high costs and the high environmental impact. In recycling of polymers products the fluorine gas contributes to destruction of ozone layer. Between 2005 and 2010, Kulikov published studies about components, which do not have the disadvantages of fluoropolymers as isocyanates and polyols, polymerized silanols and citric acid.

The present work examines the effects of PPA in extrusion of LLDPE resins. By determining how efficiently the PPA eliminated sharkskin in a LLDPE on a blown film extruder and capillary extruder. Three formulations of PPA from different suppliers were studied.

It was also analysed the optical and mechanical characteristics of film with smooth surface and with defects, as sharkskin, vertical lines and gel.

2. Experimental

2.1. Materials

The resins of polyolefin used was LDPE having a melt flow index (MFI) of 0.85 g/10min and density of 922 kg/m^3 and LLDPE is characterized by MFI of 1 g/10min and density of 918 kg/m^3.

The three formulations of PPA used are manufactured by different companies. The PPA used by the company Isolago S.A. which to produces masterbatch (MB) is named PPA-1 and the other two PPA are named PPA-2 and AP-3. The MB of PPA-1 is named PPA-1MB. The concentration of PPA in the masterbatch was 2%.

2.2. Extrusion equipment/Procedure

The blown film extruder (Fivex) is a single screw extruder with a 29:1 L/D (length/diameter), 3.6 cm of die diameter and a die gap of 0.1 cm.

The capillary extruder (Collin) is a single screw extruder with 25:1 L/D. The initial diameter of the die is 2 cm and at the end has a small downward curvature with diameter of 0.3 cm. The extruder has a melt pump in the die. The speed was held at 50 rpm.

In blown film extrusion, temperature set points from feed zone to die zone, were 150/160/170/170/170 ºC. The nip rolls speed allows the film to rise 2.7 m/min. In capillary extrusion temperature set points from feed zone to die zone, were 40/170/200/200/200/200 ºC. In both extruders the speed was held at 50 rpm.

Tests with pure polyethylene: Pure LDPE was extrude for 30 minutes and pure LLDPE was extruded for 60 minutes. With LLDPE the time was longer because the pressure instability was greater. The pressure and intensity of the engine were recorded.

Tests with PPA/LLDPE: First, pure LLDPE was extruded until obtain sharkskin. Next, PPA/LLDPE blend was extruded. The concentration of PPA in the blend was 0.04%. The time to eliminate sharkskin (during the extrusion of PPA/LLDPE blend), pressure and intensity of the motor were recorded. The tests were stopped when the pressure stabilized. Film sampes were taken during the tests. After each test, the equipment was purged using a mass fraction of 80 % of calcium carbonate masterbatch in LLDPE this helped remove traces of PPA and others contaminants.

2.3. Optical microscope/Procedure

The optical microscope (Leitz Orthoplan®) and the microscope digital camera (Motic®, Moticam 10.0 MP) using the software Motic Images Plus 2.0. were used to observe and obtain images of film surface defects (vertical lines, gel, sharkskin). Film samples were cut and glued on glass slide. Then the samples were put on specimen stage in the vertical direction relative to operator and the images were observed. It was used a magnification of 63x.

The birefringence was calculated for film with gel, by ration of retardation and film thickness. The value of retardation was obtained by observation of the interference colour of the film (with crossed polarizers at position of maximum brightness) by Michel-Lévy interference colour chart. The position of maximum brightness corresponds at rotation of 45º of specimen stage from position of extinction.

2.4. Electron microscope/Procedure

The scanning electron microscope (JEOL JSM-7001F) with a resolution of 1.2 nm at 15 kV was used to observe the microstructural changes caused by film defects. Comparing films with smooth surface and with defects (sharkskin and gel). It was used a magnification of 3500x.

2.5. DMA/Procedure

Dynamical mechanical experiments were performed using TA Instruments Q800 DMA in film tension mode. The software QSeries™ controls the parameters of the tests.

Samples of LDPE film and LLDPE film, with smooth surface and with defects (sharkskin and gel) were used in the tests. Smooth surface films samples were obtain after extrusion with AP-1, AP-2, AP-3 and AP-1MB. Also, it was analysed film with smooth surface obtain without PPA, the sample is named pure LL.

Dynamic measurements: samples were analysed using a strain amplitude of 15 µm at a multi frequency mode, using 3, 1, 0.3 and 0.1 Hz. A dynamic temperature ramp of 1ºC/minute was used for a range of approximately 25ºC to 100 ºC. The static force applied was 0.08N.

The storage modulus (E´), loss modulus (E´´) and loss factor tan δ were measured for each frequency as the temperature increases.

Creep recovery test: It was applied a constant tension of 3 MPa (residual static force of 0.001 N and static force of 1.3 N) at creep time and the tension was removed at recovery time.

At 35 ºC creep time was 180 minutes and recovery time was 300 minutes. At 60 ºC creep time was 20 minutes and recovery time 50 minutes.

The strain, $\gamma(t)_{experim.}$, and mechanical compliance, J(t), were obtained.

2.6. FTIR/ Procedure

It was used the infrared spectrometer with Fourier transform (Perkin Elmer®) and the software Perkin Elmer Spectrum to analyse and compare infrared spectrums of PPA.
Powder samples of PPA were distributed in different mortars with potassium bromide and were mixed and grinded with the pestle. Then the mixture was pressed in manual press (10 tonnes/cm^2 for 5 minutes) to form a transparent pellet. This allows the infrared radiation through the sample in the spectrometer.

3. Results and discussion

3.1. Extrusion of pure LDPE and pure LLDPE

Pressure and intensity of the process were higher with LLDPE. Output was higher in LDPE extrusion, at the 50 rpm. The values recorded in blown film extrusion and capillary extrusion are in Table 1.

The results indicates that the LDPE resin used has lower viscosity than LLDPE. Since pressure increases with polymer melt viscosity.

Table 1- Pressure, intensity and output in extrusion.

Extrusion	Type polyethylene	Pressure (Bar) max./min.	Intensity (Amperes) max./min.	Output (g/min)
Blown film	LDPE	37/41	4.9/5	53.9
	LLDPE	44/51	5.8/6	50.9
Capillary	LDPE	17/18	2.5	23.0
	LLDPE	24-25	2.9	19.5

3.2. Extrusion of LLDPE with PPA

Processing LLDPE with PPA pressure decreases over time, because flow instabilities are reduced while PPA coats the die wall.

In blown film extrusion was observed pressure and intensity reduction. In capillary extrusion the pressure was stable (probably because of the melt pump) but was observed intensity reduction.

The intensity reduction in both extruders was similar for all tests. So it is not possible qualify which PPA formulations have more contribution to intensity reduction.

The pressure reduction percentage was 24, 19, 25 e 21 %, for tests with PPA-1MB, PPA-1, PPA-2 and PPA-3, respectively.

The pressure reduction was faster with PPA-1 and PPA-2 comes in second place. The pressure reduction was slowly with AP-3 and AP-1MB. The variation of pressure with time in blown film extrusion are in Figure 1.

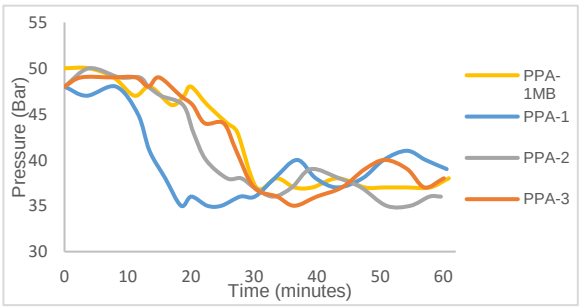

Figure 1- Variation of pressure with time in blown film extruder.

The use of PPA increase the critical flow rate. Meaning the sharkskin will appear at higher flow rate. This was confirmed with all formulations of PPA used in blown film extruder and capillary extruder. Since when pure LLDPE was extruded,

sharkskin was observed and after introducing PPA the surface becomes smooth after a certain time, at the same flow rate.

Examples of film and capillary extrudate at the beginning and at the end of the extrusion with PPA/LLDPE blend are in Figure 2.

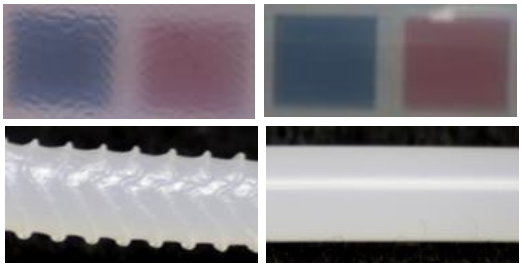

Figure 2- Film and capillary extrudate before and after PPA (Canon EOS 5D Mark II, EFS 300-700 mm).

The time to eliminate sharkskin in blown film extrusion and capillary extrusion obtained for all the tests are in Table 2. In both extruders the time to eliminate sharkskin has the same hierarchy.

Using masterbatch the time to eliminate sharkskin is the highest, probably because of the different form to incorporate PPA in the LLDPE resin. When masterbatch is used, the dispersion of PPA in the polymer melts are better.

Table 2- Time to eliminate sharkskin (minutes).

	AP-1	AP-2	AP-3	AP-1MB
Blown film extrusion	22	25	30	43
Capillary extrusion	32	34	39	44

Comparing pressure reduction (Figure 1) and time to eliminate sharkskin (Table 2), it is noticed that for longer times to eliminate sharkskin, the slower the pressure reduction. If the sharkskin removal is slow, it means that the die wall coating with AP is slow. While high wall shear stress persists the pressure will take longer to decrease

The pressure reduction and time to eliminate sharkskin are the data used to comparing efficiency of PPA.

The results indicate that PPA-1 gave the best performance of all formulations of PPA tested, although the pressure reduction percentage is the smallest. Since it is necessary less time to eliminate sharkskin and pressure reduction occurs more rapidly than the others formulations, PPA-1 can be considered the most efficient.

The second most efficient formulation is PPA-2, because the time to eliminate sharkskin is similar to the PPA-1 time and the pressure reduction is quicker than with PPA-3.

So PPA-3 formulation is considered the less efficient, because more time is necessary to eliminate sharkskin and reduce the pressure.

The presence of gels on the surface of the films was very sporadic and die build up wasn´t observed during extrusion with pure LLPDE and PPA/LLDPE blend. So it wasn´t possible determine which of the AP formulations allow more effectively to reduce these defects.

Die build up was formed at the die exit during purge in both extruders. This means the cleaning was efficient, because indicates that particles of PPA and other contaminants were removed from the die wall, i.e. calcium carbonate particles migrated easily until the die wall and separated contaminants from the wall.

3.3. Optical microscope

Before cleaning the blown film extruder many vertical lines were observed in the LLDPE film (Figure 3 (1)). After cleaning and extruding PPA/LLDPE blend, a few vertical lines were present in the film (Figure 3 (2)). This means that the vertical lines are mostly originated from accumulated and degraded polymer on the die wall. So the vertical lines observed in Figure 3 (2) must be caused by defects in the die wall.

The gel (Figure 3 (3)) has an elliptical form, because of shear forces in the die. The gel observed isn't caused by thermally degraded polymer or contamination, because it does not have a black dot in the centre, named fisheye.

Sharkskin is a periodical distortion oriented perpendicularly to the flow direction, like observed in Figure 3 (4).

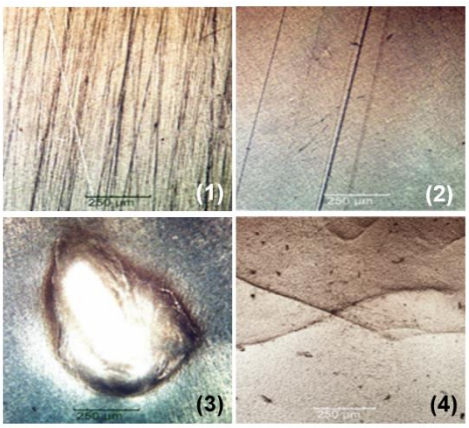

Figure 3- Surface film defects (63x).

In the film sample with gel, the interference colour in gel zone has clearer grey tone than the film. By consulting a Michel-Levy chart [6] the difference in colour indicates that birefringence is highest in

the gel zone. This means that´s in gel the polymer chains are under stress.

As the stress is increasing, so is the orientation of the polymer chains, and as a result the birefringent is also higher.

The value of birefringence obtained was 2.25x10^{-3}. Since the value of retardation considered was 180 nm and film thickness was 80 µm. The result of the birefringence wasn´t possible to confirm by using a compensator. But there is no certainty that would significantly improve the estimate of the birefringence, due to the small size of the gel.

3.4. Electron microscope

Comparing SEM images of smooth surface (Figure 4 (a)) with gel (Figure 4 (b)) and sharkskin (Figure 4 (c)) SEM images it is observed microstructural changes in films with defects.

The film with sharkskin has a periodic structure, which is associated with elastic recovery of the polymer, after being submitted to high local stresses in the surface at the die exit.

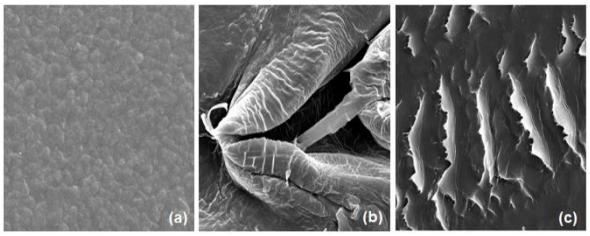

Figure 4- SEM images of smooth surface (a), gel (b) and sharkskin (c) in LLDPE films.

3.5. DMA

Dynamical measurements:

In Figure 5 are presented the variations of storage modulus (E´), loss modulus (E´´) and loss factor Tan δ with temperature, at each frequency, for the test with film sample of AP-2. In axis Y-1 and T-4 the scale is logarithmic and in axis Y-2 and Y-3 the scale is normal. The behaviour of the curves was similar in all film samples.

The variation of tan δ with temperature has a maximum. This indicates that the film sample received sufficient energy to move the polymer chains. The energy is named apparent activation energy, Ea, and is related with the temperature at the maximum of tan δ, named $T_{máx}$. The Ea is determined by slope of the equation (1). The parameter w is the frequency, w_0 is the frequency factor and R is the gas constant.

$$\ln w = lnw_0 - \left(\frac{Ea}{R}\right)\frac{1}{T_{max}} \qquad (1)$$

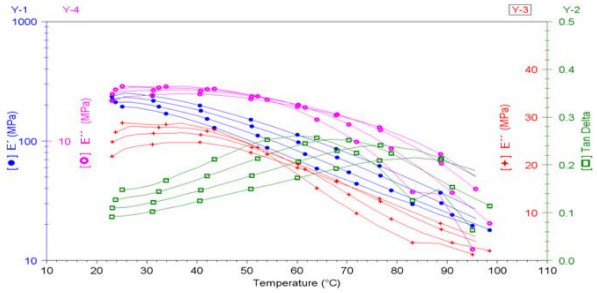

Figure 5- Variation of storage modulus, loss modulus and loss factor tan δ with temperature, test with AP-2.

The values of Ea obtained with film samples are in Table 3. The LDPE film sample has the highest value of Ea. The LDPE has long chain branching, then the movement of the chains is more difficult, because of high entanglement between the chains. Therefore in LDPE the energy required to move the chains is higher than with LLDPE.

The film sample with gel has the value of Ea higher than other LLDPE film samples. Possibly because it is more difficult to move the polymer chains in gel zone.

PPA-1MB, PPA-1, PPA-2 and pure LL film samples have similar values of Ea.

AP-3 film sample has the lowest value of Ea. It means, that less energy was required to move the polymer chains. It is not possible determine the cause of this fact, particularly the reason of being easier to move than sharkskin sample.

Table 3- Values of apparent action energy in LDPE and LLDPE films.

Film sample	**PPA-1MB**	**PPA-1**	**PPA-2**	**PPA-3**
Ea (kJ/mol)	140.40	144.44	140.38	133.98
Film sample	**Gel**	**Pure LL**	**Sharkskin**	**LDPE**
Ea (kJ/mol)	148.31	145.46	135.81	189.57

Creep recovery tests:

In a creep recovery experiment a stress is applied for a particular period of time (creep time) and the sample is deformed. After creep time the stress is removed and the sample tend to recuperate the initial dimensions during a specific time (recovery time). Usually with a viscoelastic material, like polymers, only elastic deformation is recovered during recovery time. The viscous deformation isn´t recovered, so it´s characterized as irreversible deformation.

The mechanical compliance, J(t) , characterizes the deformation of the material. The higher the J(t), the greater the strain of the material.

The curves of J(t) obtained by the equipment didn't show the expected behaviour. So it was necessary to determine the values of J(t) by equation (2) at creep time $t_0<t<t_1$ and recovery time $t>t_1$. J_0 is the instantaneous compliance, J_{di} is the retarded compliance, λ_i is the retardation time, β_i is a adjustment parameter. The ratio t/η is the irreversible compliance ($J_{irrev.}$) and can be despised if the material is a solid, because the viscosity (η) is considered infinite.

To determine the parameters (J_{di}, λ_i and β_i,) was necessary to approximate the values of total strain, $\gamma(t)_{total}$, to the values of experimental strain, $\gamma(t)_{experim.}$. The total strain consist in all values of creep strain (equation (3)) and recovered strain, equation (4).

$$J(t) = J_0 + \sum_i J_{di}\left(1 - e^{-\left(\frac{t}{\lambda_i}\right)^{\beta_i}}\right) + \frac{t}{\eta} \quad (2)$$

$$\gamma(t)_{creep} = J_0\sigma_0 + \sigma_0 \sum_i J_{di}\left(1 - e^{-\left(\frac{t-t_0}{\lambda_i}\right)^{\beta_i}}\right) \quad (3)$$

$$\gamma(t)_{recov..} = \sigma_0\left(\sum_i J_{di} e^{\left(\frac{t-t_1}{\lambda_i}\right)^{\beta_i}} - \sum_i J_{di} e^{-\left(\frac{t-t_0}{\lambda_i}\right)^{\beta_i}}\right) \quad (4)$$

The curve formed by the values of $\gamma(t)_{total}$ was adjusted to the values of $\gamma(t)_{experim.}$ by Solver tool of Microsoft Office Excel, changing the parameters (J_{di}, λ_i and β_i, i=1 to i=3) until obtain the value of chi-square test (χ^2, equation (5)) with the lowest possible. O_i is the observed value ($\gamma(t)_{total}$) and E_i is the expected value ($\gamma(t)_{experim.}$).

$$\chi^2 = \sum_i \frac{(O_i - E_i)^2}{E_i} \quad (5)$$

This procedure was done for all film samples at 35 ºC and 60 ºC, with J_0 of $1x10^{-10}Pa^{-1}$.In Figure 6 is observed the curve of total strain and values of experimental strain, for PPA-1 film sample at 35 ºC. The curves I, II and III correspond to partial deformations delayed, i = 1 to i = 3.

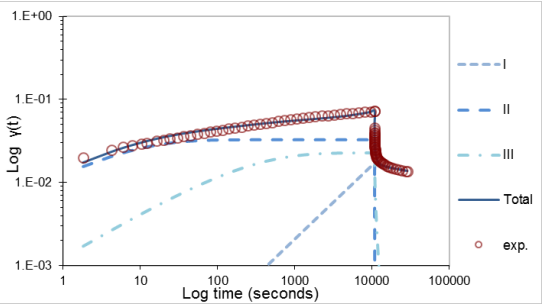

Figure 6- Total strain, experimental strain vs time, for AP-1.

The wide distribution of retardations times that were obtained facilitates interpretation. The shorter the retardation time, the faster the deformation occurs. For all film samples, at 35 ºC and 60 ºC, the orders of magnitude are approximately of 0 for λ_1 , 1 for λ_2 and 7 for λ_3.

The λ_1 may be related with the motion in amorphous region, because the motions are easy due to the disorder of polymer chains. So it takes a short time until deform.

The λ_2 may be related with the motion in crystalline region, because the motion of polymer chains in a ordered region is more difficult than in the amorphous region. So the deformation is slower. The λ_3 is considered infinite and may be related with irreversible deformation.

The parameter β_i may be related to the molecular cooperativity of polymer chains. Which corresponds to chain movement, due to the interaction with the movement of the neighbouring chains.

According to *Ngai* e *Roland* [7] the polyethylene is considered one of the polymers with less intermolecular cooperativity, because has symmetrical chain backbones and hasn´t bulky or polar groups. So in this case β_i can´t be related to the molecular cooperativity

The values of β_i obtained for all film samples are less than or equal to 1. And allowed a good approximation of the values of $\gamma(t)_{total}$ to $\gamma(t)_{experim.}$.

Without using β_i the values of χ^2 were higher than the actual values.

The variation of J(t) obtained for all film samples is in Figure 7 for experiments at 35 ºC and in Figure 8 for experiments at 60 ºC.

At 60ºC the resolution is higher than at 35 ºC i.e. the difference between J(t) curves of all film samples is greater at higher temperatures and the range of values is high.

For high temperatures the deformation of the material is higher and faster that at low temperatures, because the motion of polymer chains is easier at high temperatures. So the interpretation of J(t) is mostly based in Figure 8.

The LDPE film sample has the lowest values of J(t). So the high entanglement between the chains in LDPE (due the long chain branching) affect the deformation of the polymer.

The film sample with gel, at 60ºC, has the values of J(t) lowest than film sample with smooth surface (PPA-1, PPA-2, PPA-3, PPA-1MB and pure LL) and sharkskin, perhaps this occurs

because the orientation of polymers chains in gel affected the deformation of all sample.

The film samples with sharkskin have the highest values of J(t). Therefore the movement of the polymer chains is facilitated in the presence of sharkskin, possibly due to different organization of the polymer chains. So the sharkskin defect in film is considered the worst condition from the mechanical point of view, because the film is more easily deformed.

The most favourable condition is to get smooth film surface without applying PPA. The sample pure LL represents this situation.

The samples of film obtained after processing LLDPE with PPA have the variation of J(t) similar to pure LL sample, with the following order of approximation: AP-1MB, AP-1, AP-3 e AP-2, at 60ºC.

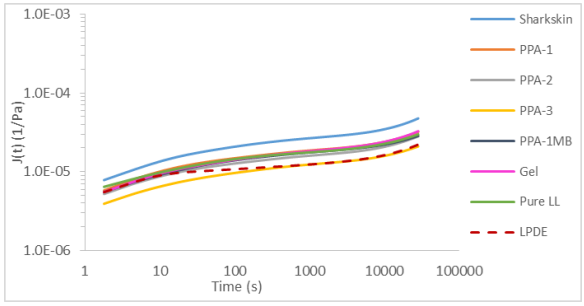

Figure 7- Variation of compliance with time at 35ºC.

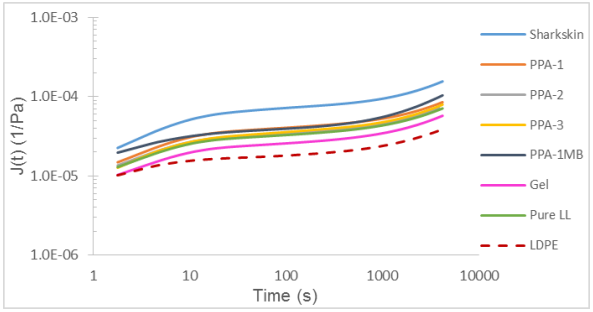

Figure 8- Variation of compliance with time at 60ºC.

3.6. FTIR

The infrared spectra (% Transmittance *vs* wavenumber) of formulations PPA-1, PPA-2 and PPA-3 obtained in the range of wavenumber of 4000 to 400 cm^{-1} are in Figure 9.

Overall between 4000 and 2000 cm^{-1} the localization of absorption bands are similar in all three infrared spectra. The absorption bands have more difference between 2000 and 400 cm^{-1} (Figure 10).

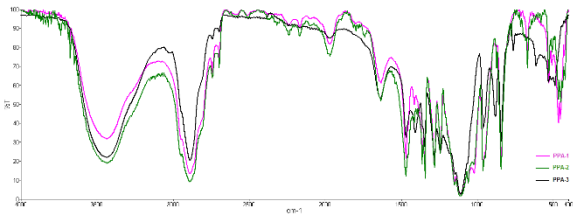

Figure 9- Infrared spectra of PPA, between 4000 and 400 cm^{-1} (pink is PPA-1, green is PP-2 and black is PPA-3).

Usually PPA are constituted by a fluoropolymer, interfacial agent (polyethylene glycol or polycaprolactone) and inorganic compounds, as calcium carbonate, silica and talc. According to suppliers of PPA the calcium carbonate, silica and talc are in very low concentrations. So in the analysis of the spectrums was ignored the presence of these components.

The identification of absorption bands of PPA is not very accurate. There are displacements and absence of absorption bands in the AP spectrums, compared to the spectrum of pure components.

The poly(vinylidene fluoride-co-hexafluoropropylene) (PVDF-co-HFP) and polyethylene glycol (PEG) are the main components of PPA. The analysis of the spectrums is based in these components.

PEG (H-[-O-CH_2-CH_2-]$_n$-OH):

By comparing the spectra absorption bands, with the PEG absorption bands (referred to in literature), it was possible to consider that some bands correspond to the vibrations of the chemical bonds of PEG.

The absorption bands observed in the spectra and as referred in the literature, with the corresponding vibrations modes (stretching υ, out-of-plane bending δ_{out} and scissoring σ) of PEG are in Table 4.

The absorption bands at 1958, 1638 and 525 cm^{-1} do not have indication of the vibration mode.

The spectra of all formulations of PPA have the absorption bands in the Table 4, so is confirmed the presence of PEG.

The absorption band at 1730 cm^{-1} related to vibration of C=O, does not appear in the spectra. If it were in the spectra the component was oxidized. So the PEG is in good conditions.

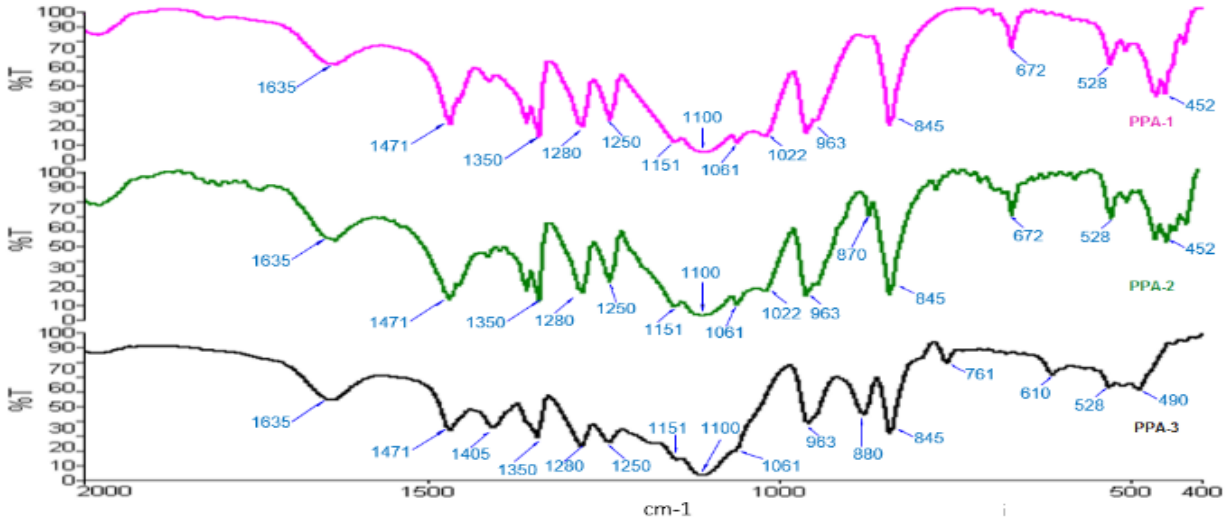

Figure 10- Infrared spectra of PPA, between 2000 and 400 cm^{-1}.

Table 4- Wavenumber and vibration mode of PEG

Wavenumber (cm^{-1})		Vibration mode
References	Spectra	
3570-3200 [8]	3350	υ (O-H)
2890 [8]	2890	υ (C-H)
1958 [9]	1958	-
1638 [9]	1635	-
1471 [9]	1471	σ (C-H)
1343 [9]	1350	δ_{out} (C-H)
1279 [8]	1280	υ (C-O-H) e υ (O-H)
1240 [9]	1250	υ (C-O-C)
1150 [9]	1151	υ (C-O-C)
1100 e 1094 [8]	1100	υ (C-O-H) e υ (O-H)
970-960 [8]	963	δ_{out} (C-H)
890-800 [9] e 840 [9]	845	υ (C-O)
525 [8]	528	–

PVDF-co-HFP, $-(-CH_2-CF_2-)_x-(-CF_2-CFCF_3-)_y-$:

In the infrared spectrum is possible to differentiate absorption bands corresponding to the crystalline and amorphous region of the fluoropolymer. The VDF (polyvinylidene fluoride) monomer is mostly related with crystalline region and HFP (hexafluoropropylene) monomer with amorphous region.

The absorption bands relating to polymorphic crystalline forms of VDF, such α and β, can be identified in the spectrum.

The absorption bands observed in the spectra and referred in the literature, with the corresponding vibrations modes (stretching υ, symmetric stretch υ_s, antisymmetric stretch υ_a, bending δ, wagging w and rocking ρ) of PVDF-co-HFP are in Table 5.

There are absoption bands referred in literature but missing in spectra of PPA. Possibly due the displacement of bands or because the bands are hidden in neighboring bands.

The absorption bands in PPA-1 and PPA-2 spectra are similar. But the absorption band at 870 cm^{-1} only appears in PPA-2 spectrum. Possibly this band is occult in the absorption band at 845 cm^{-1} in PPA-1.

The absorption bands at 1022, 672 and 452 cm^{-1} only appears in PPA-1 and PPA-2 spectrum.

The absorption band at 672cm^{-1} it is not referred in literature. Possibly it was originated from the displacement of the band at 615 cm^{-1}.

The PPA-3 spectrum has absorption bands which does not appear in PPA-1 and PPA-2 spectra. For example the absorption bands at 1405, 761, 610 e 490cm^{-1}, related to crystalline form α.

The absorption band at 880 cm^{-1} only appears in PPA-3 spectrum. But in PPA-2 spectrum the absorption band at 870 cm^{-1} corresponds to the same vibrations modes.

The PPA-3 spectrum has more absorption bands related to crystalline region than PPA-1 and PPA-2 spectra. So it is possible to consider that the formulation PPA-3 has the PVDF monomer in higher quantity. Therefore the difference between the spectra are related to the different proportions of the monomers, in the copolymer. Then the proportions of the monomers in formulations PPA-1 and PP-2 are the same, because of the similarity of the spectra.

It is also possible to consider that PVDF-co-HFP is a block copolymer or alternating copolymer.

In the spectra the absorption bands related to the crystalline region are more or less well defined. This indicated that the copolymer has an organized structure, which facilitates the crystallization.

Table 5- Wavenumber and vibration mode of PVDF-co-HFP

	Wavenumber (cm^{-1})				Vibration mode
	References			Spectra	
-	-	-	450 [10]	452	w (CF_2)
	-	-	106 [11]	1061	υ (CF_2)
	-	-	1069 [10]	-	δ (CF_3)
	-	1179[11]	1179 [10]	-	υ_s (CF_2)
	-	-	1203[11]	-	υ_a (CF_2)
	-	-	1383[11]	-	w (CH_2)
	-	-	1022 [8]	1022	υ (C-F)
	-	-	2989-2911 [10]	2890	υ (CH_2)
α	-	-	489 [12]	490	δ (CF_2)
	-	530 [13]	534 [12]	528	δ (CF_2)
	-	615 [13]	614 [12]	610	δ (CF_2)
		761[10]	762 [12]	761	δ (C-C)
	-	795 [13]	796 [12]	-	ρ (CH_2) and/or υ (CF_3)
	974[11]	986 [10]	976 [12]	-	υ (C-F)
	-	1401 [11]	1402 [10]	1405	w (CH_2) and/or υ (C-F)
β	-	-	509 [13]	511	δ (CF_2)
	840[13]	842 [10]	840 [12]	845	ρ (CH_2)
*	871 [11]	873 [11]	880 [12]	870/880	υ_s (CF_2) and/or υ_s (C-C)

*Amorphous region

4. Conclusions

The results of processing pure resins of LDPE and LLDPE shows that the melt LDPE flows more easily through the die. Because the pressure it was lower and the output was higher. So this indicates that the LDPE resin used has lower viscosity than LLDPE.

In blown film extrusion, the elimination of film defects (in the optical point of view) and the pressure stabilization are related. When the sharkskin was eliminated the pressure began to stable.

The critical flow rate increased during the processing of LLDPE resin with all formulations of PPA used. Because using PPA, at constant flow rate the sharkskin did not appear after a certain time. This time is defined as a time to eliminate sharkskin. With the formulations PPA-1, PPA-2 and PPA-3 the values of time obtained were different.

The formulation PPA-1 is considered the most efficient. Because the time to stabilize the pressure and eliminate the sharkskin was the lowest. This means the formation of a die coating occurs more rapidly than the others formulations.

Using PPA-1 there is less waste of polymer extrudate (without quality) and the operations conditions are more favourable (lowest pressure). The formulation PPA-2 is considered the second most efficient. Since the time to eliminate sharkskin was the second shorter and the pressure stabiles more rapidly than with PPA-3. Thus PPA-3 of all formulations analysed is considered the less efficient. The time to eliminate sharkskin is the highest and the pressure takes more time until stabilize.

It was shown that die build up is useful for die cleaning. If there is die build up during cleaning, this mean there is elimination of accumulated material at the die wall.

In the optical microscope the defect of the film vertical lines was observed. After cleaning the extruder, where die build up was formed, was observed only a few vertical lines on the film. This indicates that vertical lines are associated with the precursor phenomenal of die build up.

Also with the optical microscope was possible to verify that the gels present on film aren´t fisheyes. It means there was an efficient fusion of polymer pellets and absence of thermally degraded polymer or other type of contamination.

It was shown by analysis of the birefringence in the film, that in the gel zone the polymer chains were possibly under stress, so were more oriented.

So the microstructural changes observed on SEM images of gel, possibly are related with the highest orientation of polymers chains.

The results of dynamical measurements and creep recovery tests, indicate that LDPE film has higher resistance to deformation. Due the long chain branching. The apparent activation energy obtained was the highest and the values of mechanical compliance were the lowest.

The DMA results for film sample with gel show that the motion of polymer chains is more difficult, consequently the hardest the deformation of the sample. Possibly because the polymer chain are under stress, as the birefringence indicates. The apparent activation energy is the highest and the values of mechanical compliance (at 60ºC) are the lowest of all samples of LLDPE film.

The mechanical compliance results for film with sharkskin indicate that the film has low resistance to deformation. The mechanical compliance values are the highest.

The PPA-2 sample probably has the most favourable mechanical properties, because the variation of J(t) is most similar to pure LL sample.

Analysing the infrared spectra was confirmed the presence of PEG in all PPA formulations.

The PPA-1 and PPA-2 spectra have identical absorption bands related to the PVDF-co-HFP. It was considered that the proportions of the monomers are the same.

The PPA-3 spectrum has more absorption bands related to PVDF monomer. So the formulation PPA-3 has the proportions of the monomers have a different formulation then PPA-1 and PPA-2.

It should be noted that there is a relationship between the analysis of the infrared spectra and the efficiencies considered for the formulations of PPA.

The PPA-1 and PPA-2 spectra are similar, and formulations are considered the most effective. While PPA-3 it's considered the less efficient formulation, and his spectrum has some absorption bands different the PPA-1 and PPA-2 spectra.

Probably when the PVDF monomer it's present in high quantity, the affinity of the fluoropolymer with the material of the die wall is slightly reduced. As a result takes longer to coat of the die wall.

5. References

[1] Qenos. (2015). *General Properties – Techical guide.* Acedido a 11 de Dezembro de 2015, em: http://www.qenos.com/internet/home.nsf/(LUImages)/TG1GenProp/$File/TG1GenProp.pdf

[2] Hatzikiriakos, S.G. and Migler, K.B. (2005). Polymer processing instabilities, Control and understanding. Marcel Dekker. New York.

[3] Kulikov, O. (2005). Novel processing aid for extrusion of polyethylene. Journal of vinyl & additive technology. 11: 127-131.

[4] Hornung, K. and Kulikov, O. (2006). Novel processing aid based on modified Silly Putty®. Journal of vinyl & additive technology. 12: 131-142.

[5] Hornung, K., Kulikov, O., and Wagner M. (2010). Low viscous hydrophilic processing additives for extrusion additives for extrusion of polyethylene at reduced temperatures. Polymer engineering and science. 50: 1236-1252.

[6] Davidon, M. W., Fellers, T.J., Murphy, D.B. and Spring, K.R. (2004). *Introduction to optical birefringence*. Acedido a 26 de Janeiro de 2016, no web site da: Nikon Microscopy em: http://www.microscopyu.com/articles/polarized/birefringenceintro.html

[7] Ngai, K. L. and Roland, C. M. (1993). *Chemical Structure ans Intermolecular Cooperativity: Dieletric Relaxations Results.* Macromolecules. 26: 6824-6830.

[8] Coates, J. (2000). *Intrepertation of Infrared Spectra, A Practical Approach.* Encyclopedia of Analytical Chemistry. R.A. Meyers (Ed.) John Wiley & Sons Ltd. 10817-10837.

[9] Abdollahi, Y., Ahmad, M.B., Jahangirian, H., Jazayeri, S.D., Mahdavi, M., Sedaghat, S., Shabanzadeh, P. and Shameli, K., e (2012). *Synthesis and Characterization of Polyethylene Glycol Mediated Silver Nanoparticles by the Green Method*. International Jornal of Molecular Sciences. 13: 6639-6650.

[10] Sim, L.N., Majid, S.R. and Arof, A.K. (2011). *FTIR studies of PEMA/PVdF-HFP blend polymer electrolyte system incorporated with LiCF3SO3 salt.* Vibrational Spectroscopy. 58: 57-66.

[11] Ataollahi, N., Ahmad, A., Hamzah, H., Rahman, M.Y.A. and Mohamed N.S. (2012). *Preparation and Characterization of PVDF-HFP/MG49 Based Polymer Blend Electrolyte*. International Jounar of Chemical Science. 7: 6693-6703.

[12] Shalu, Singh, V.K., and Singh, R.K. (2015). *Development of ion conducting polymer gel electrolyte membranes based on polymer PVdF-HFP, BMIMTFSI ionic liquid and the Li-salt with improved electrical, thermal and structural properties*. Journal of Materials Chemistry C. 3: 7305-7318.

[13] Blottière, B. (2012). *Ternary Diagrams of Poly(vinylidene fluoride) and Poly[(vinylidene fluoride) cohexafluoropropene] in Propylene Carbonate and Dimethyl Sulfoxide.* Macromolecular Chemistry and Physics. 213: 587-593.